Bone 127 (2019) 188–198

Contents lists available at ScienceDirect

Bone

journal homepage: www.elsevier.com/locate/bone

Full Length Article

In situ cell cycle analysis in giant cell tumor of bone reveals patients with elevated risk of reduced progression-free survival

Mate E. Maros[a,b], Sven Schnaidt[c], Peter Balla[a], Zoltan Kelemen[a], Zoltan Sapi[a], Miklos Szendroi[d], Tamas Laszlo[e], Ramses Forsyth[f], Piero Picci[g], Tibor Krenacs[a,*]

[a] 1st Department of Pathology and Experimental Cancer Research, Semmelweis University, Budapest, Hungary
[b] Department of Neuroradiology, Medical Faculty Mannheim, University of Heidelberg, Mannheim, Germany
[c] Institute of Medical Biometry and Informatics, University of Heidelberg, Heidelberg, Germany
[d] Department of Orthopedics, Semmelweis University, Budapest, Hungary
[e] Department of Oto-Rhino-Laryngology, Head and Neck Surgery, Semmelweis University, Budapest, Hungary
[f] Department of Anatomic Pathology, University of Brussels, Belgium
[g] Laboratory of Experimental Oncology, Institute of Orthopedics Rizzoli, Bologna, Italy

ARTICLE INFO

Keywords:
Giant cell tumor of bone
Neoplastic stromal cells
Mononuclear cell cycle fractions
Tumor progression
ploidy
mcm2
Cyclin D1
Cyclin A

ABSTRACT

Objective: Giant cell tumor of bone (GCTB) is a frequently recurring locally aggressive osteolytic lesion, where pathological osteoclastogenesis and bone destruction are driven by neoplastic stromal cells. Here, we studied if cell cycle fractions within the mononuclear cell compartment of GCTB can predict its progression-free survival (PFS).

Methods: 154 cases (100 primaries and 54 recurrent) from 139 patients of 40 progression events, was studied using tissue microarrays. Ploidy and in situ cell cycle progression related proteins including Ki67 and those linked with replication licensing (mcm2), G1-phase (cyclin D1, Cdk4), and S-G2-M-phase (cyclin A; Cdk2) fractions; cell cycle control ($p21^{waf1}$) and repression (geminin), were tested. The Prentice-Williams-Peterson (PWP) gap-time models with the Akaike information criterion (AIC) were used for PFS analysis.

Results: Cluster analysis showed good correlation between functionally related marker positive cell fractions indicating no major cell cycle arrested cell populations in GCTB. Increasing hazard of progression was statistically associated with the elevated post-G1/S-phase cell fractions. Univariate analysis revealed significant negative association of poly-/aneuploidy ($p < 0.0001$), and elevated cyclin A ($p < 0.001$), geminin ($p = 0.015$), mcm2 ($p = 0.016$), cyclin D1 ($p = 0.022$) and Ki67 (B56: $p = 0.0543$; and Mib1: $p = 0.0564$ –strong trend) positive cell fractions with PFS. The highest-ranked multivariate interaction model (AIC = 269.5) also included ploidy (HR 5.68, 95%CI: 2.62–12.31, $p < 0.0001$), mcm2 ($p = 0.609$), cyclin D1 (HR 1.89, 95%CI: 0.88–4.09, $p = 0.105$) and cyclin A ($p < 0.0001$). The first and second best prognostic models without interaction (AIC = 271.6) and the sensitivity analysis (AIC = 265.7) further confirmed the prognostic relevance of combining these markers.

Conclusion: Ploidy and elevated replication licensing (mcm2), G1-phase (cyclin D1) and post-G1 phase (cyclin A) marker positive cell fractions, indicating enhanced cell cycle progression, can assist in identifying GCTB patients with increased risk for a reduced PFS.

1. Introduction

Giant cell tumor of bone (GCTB) is a locally aggressive lesion caused by pathological osteolysis predominantly affecting the epi-metaphyseal bone regions in young adults, which represents ~5% of the primary and ~20% of benign bone tumors, with the highest range observed in the Asian population [1–3]. Despite appropriate treatment, GCTB may frequently (in 20–50%) show local recurrence, and rarely the tumor spreads as "metastatic" emboli to the lung (in 1–4%), or show malignant transformation in 1–4% [4–8]. However, the clinical progression of GCTB cannot be predicted from histopathological features. Though several biomarkers of chromosomal instability, cell growth signaling and tumor microenvironment have been tested with promise, none of these became part of the daily diagnostic routine [8–13]. Since elevated

* Corresponding author at: 1st Department of Pathology and Experimental Cancer Research, Semmelweis University, Ulloi ut 26, H1085 Budapest, Hungary.
E-mail address: krenacst@gmail.com (T. Krenacs).

https://doi.org/10.1016/j.bone.2019.06.022
Received 4 February 2019; Received in revised form 23 May 2019; Accepted 21 June 2019
Available online 22 June 2019

cell replication is often associated with aggressive tumor behavior and poor disease prognosis [14], here we studied if testing of cell cycle fractions in the mononuclear cell compartment can help predict GCTB progression and prognosis.

In GCTB, osteoclast type giant cells are admixed with mononuclear cells including the osteoclast precursor monocytic/macrophage lineage cells and stromal cells of osteoblastic origin [4,15]. Abnormal osteoclastogenesis is thought to be driven by these stromal cells which are considered to be neoplastic [16] due to their chromosomal instability [17], telomeric associations [18], elevated proliferative activity [12], and H3F3A (H3 Histone Family Member 3A) gene mutations in > 90% of the cases (dominantly at Gly34) [13,19,20]. Neoplastic stromal cells express early osteoblast markers [21] and secrete cytokines, which regulate osteoclastogenesis including macrophage colony stimulating factor (M-CSF), interferon-gamma (IFNγ), and the tumor necrosis factor (TNF) family ligand RANKL (receptor activator of nuclear factor kappa) [4,15,22]. Earlier we found an increased hazard of progression in GCTB cases presenting elevated epidermal growth factor receptor (EGFR) expression [7] or reduced and deregulated gap junction connexin43 (Cx43) channels in the neoplastic stromal cell fractions [10].

Accelerated cell cycle progression has been linked to genomic instability, elevated tumor grade and aggressiveness resulting in worse clinical outcome in breast [23], colorectal- [24] and lung adenocarcinomas [25], epithelial ovarian carcinomas [26] as well as in melanomas [27], and in Ewing's Sarcoma Family of Tumors (ESFT) [28]. Proteins regulating cell replication can be detected [29] in situ using immunohistochemistry for the assessment of cell cycle fractions in archived tissues [30]. For entering the cycle, a restriction point needs to be bypassed [31] at early G1 phase [32] by licensing, which involves the minichromosome maintenance 2–7 (mcm2–7) complex [33–35]. Besides Ki-67, mcm2–7 complex proteins can be detected throughout the cycle except in quiescence (G0) thus, they can be used as general markers of tumor growth fractions [30,33,36,37]. Complexes of cyclins and cyclin-dependent serine-threonine kinases (cdk) drive the cells through major phases of the cycle [38]. The cyclin D1-cdk4/6 complex promotes G1/S-phase transition by phosphorylating retinoblastoma (Rb) protein [39,40], which can be prevented either by $p16^{INK4}$ [41] and $p21^{waf1}$ cdk inhibitors [38,42–44]. The cyclin A-cdk2 complex drives S/G2 phase transition [29], while in late G2 phase cyclin A also binds to cdk1 and to support G2/M phase transition [14,45]. Concurrently, geminin -a DNA replication repressor- prevents repeated replication licensing in post-G1 phase [23,36,46,47]. Finally, the cyclin B1-cdk1 complex catalyzes mitotic cell division [48] by activating the microtubule assembly and chromatin and DNA relaxation for increased gene transcription through phosphorylating H1 and H3 histones. Failure of cytokinesis during mitosis (M-phase) can result in poly- or aneuploidy, which contribute to chromosomal instability and the development and progression of tumors [49]. The tumor suppressor p53 can induce cell cycle arrest by upregulating $p21^{waf1}$ expression and DNA damage response [50].

Elevated cell proliferation has already been linked to GCTB progression, however, so far only small patient cohorts have been tested using either only general proliferation markers or those expressed only at early phases of the cycle [12,51–53]. On the other hand, recurrence potential in a larger cohort was controversially linked to p53 and cyclin D1 upregulation in mononuclear and giant cells, respectively [54]. The link between mononuclear cell cycle fractions and progression-free survival (PFS) in GCTB has not been properly investigated yet.

Since GCTB can lead to substantially reduced quality of life or even death, it is crucial to identify patients with increased risk of recurrence. In this study we correlated the proliferating mononuclear cell fractions with PFS in tissue microarrays (TMA) of 154 GCTB cases from 139 patients using immunohistochemistry through detecting nuclear cell cycle regulation-linked proteins in the osteoclast rich regions. The DNA index (ploidy) was also determined and considered in the analysis.

2. Materials and methods

2.1. Study cohort

A single-center retrospective cohort study was performed in formalin-fixed and paraffin-embedded GCTB samples, which were surgically removed and diagnosed between 1994 and 2005 at the Institute of Rizzoli, Bologna (IOR), Italy. All adult patients or both parents/guardians of minors have provided a written informed consent. The study was approved by the Ethical Committees for Human Research both at Semmelweis University, Budapest (87/2007) and at the Institute of Orthopedics Rizzoli, Bologna (13351/5-28-2008).

The study included 139 patients, who underwent altogether 154 operations. Each of these excised samples were considered “surgical cases”, which were originated from 100 primaries, 37 first-, 16 second-/or higher ranked recurrences and one from lung metastasis. A total of 40 progression events, detailed in Table 2 and Table 3, including recurrences, malignant transformation, metastases and few deaths occurred during follow-up period (median: 85 months, range: 1–340 months/28.3 years), which were used in PFS analysis. TMA blocks containing duplicate, or triplicate tissue cores of 2 mm diameter were created using the TMA Master instrument (3DHISTECH, Budapest, Hungary). The surgical staging (1–3) by Enneking [55] or the radiological staging by Campanacci et al. [56], both compatible with the clinical latent, active and aggressive stages were available for all cases. As a first treatment 74 (53.2%) patients underwent curettage supplemented with local adjuvants (primarily phenol, 65/74), fifty (36.0%) tumors were resected (with wide margin 42/50), 3 excised and 1 amputated while 11 (7.9%) patients received additional radiotherapy. Detailed clinicopathological-, follow-up and survival data of the studied cases are summarized in Tables 1–3, respectively.

2.2. Immunohistochemistry

Immunostaining of cell cycle proteins was done as previously described [10,27]. Briefly, 4 μm thick sections were cut from TMA blocks and mounted onto charged adhesive slides (SuperFrost Ultra Plus, Thermo-Erie, Budapest, Hungary). For antigen retrieval the dewaxed slides were boiled either in a pH 6.1 target retrieval buffer TRS (Dako, Glostrup, Denmark) for Ki-67 (clones Mib-1 and B56) and cdk4, or in a pH 9.0 buffer of 0.01 M Tris–0.1 M EDTA (TE) for all other antibodies at ~105 °C for 30 min using an electric pressure cooker (Avair Ida, YDB50-90D, Biatlon, Pecs, Hungary). Endogenous peroxidase activity was quenched using 0.5% hydrogen peroxide in methanol for 20 min. Tissue-bound antibodies were detected using the NovoLink polymer peroxidase kit (Leica-NovoCastra, Newcastle Upon-Tyne, UK) [57]. Briefly, the TMA slides were treated in humidity chambers at room temperature with a protein block solution for 10 min and then with the primary antibodies including monoclonal anti-Ki-67 (clones MIB-1, SP6, B56), mcm2, cdk4, cyclin D1, cyclin A, cdk2, geminin, phosphohistone H3 and $p21^{waf1}$, overnight (~16 h). Antibody specifications, dilutions used and the relative expression of these markers during the replication cycle are summarized in Suppl. Table 1. Both the post-primary reagents and the polymer-peroxidase complex were applied for 30 min. Between incubation steps the slides were washed for 2 × 3 min in 0.01 M pH 7.4 Tris-buffered saline (TBS) containing 0.1% Tween 20 [27]. Peroxidase activity was revealed using a hydrogen peroxide/diaminobenzidine (DAB) substrate-chromogen kit for 3–5 min. For double labelling DAB-peroxidase reactions were combined with 3-amino-9-ethylcarbazole (AEC)-peroxidase reactions. For eliminating previously used immunosequences and thus preventing unwanted cross reactions when primary antibodies of the same species were combined, a 5 min boiling of slides in TE buffer was performed between the consecutive immunoreactions [10]. Finally, the slides were counterstained with hematoxylin and coverslip mounted using Faramount (Dako).

Table 1
Clinicopathological features of the studied cases.

Number of patients	139				
Number of cases	154				
TMA samples (cores)	215				
Single case [core]/patient	77 (35.8%) of 77 patients				
Total number of cases	157 (i.e. 77 + 23 + 56 + 1)				
Excluded missing or incomplete follow-up data	3 (1.9%)				
Progression Groups	**Number**	**Enneking's/Campanacci's staging**			
Primary	100	La 36	Ac 27	Ag 37	
1st Recurrent cases	30	La 5	Ac 8	Ag 17	
2nd Recurrence	8	La 1	Ac 5	Ag 2	
3rd Recurrence	1	La -	Ac -	Ag 1	
Median age (at 1st ever diagnosis, $n = 139$)	31.0 years (range: 5.3–76.7 years;)				
Gender (male/female)	62/77				
Gender ratio	0.805:1 (M/F) or 1:1.242 (F/M)				
Survival					
Median disease free survival	73.3 months (range: 1–170.4, LQ-UQ: 25.0–95.8 months)				
Number of progression events	40				
Localization	**Total**	**Rate (%)**	**Freq/Rank**	**Side**	
Femur	47	33.8%	1st	L15	R32
Tibia	38	27.3%	2nd	L21	R17
Sacrum + Spine|Pelvis	22	15.8%	3rd	12 + 4|	6
Radius	13	9.4%	4th	L9	R4
Other	20	14.4%	–	–	–
Upper Limb	28	20.1%			
Lower Limb	89	64.0%			
Mid-line (pelvis, sacrum, spine)	22	15.8%			
All	139				
Treatment types					
Curettage	74				
	All	LA	MM	BC	MM + BC	Other
+ Local adjuvant [LA] (phenol)	65	3	34	12	15	1
+ Methyl-methacrylate [MM]	3	–	2	1	–	–
+ Bone chips [BC]	4	–	–	4	–	–
+ Other (cryo, embolization etc.)	2	–	–	–	–	2
Resection|Amputation|Excision	54					
Wide resection	42					
Intralesional resection	2					
Marginal resection	6					
Excision|amputation	3|1					
Radiotherapy	11					
+ curettage + 40-44|40 + 30 Gy	2|1					
+ curettage + phenol + 40–56 Gy	7					
+ intralesional resection + 44 Gy	1					

GCTB: giant cell tumor of bone; L: left; R: right; La: latent; Ac: active; Ag: aggressive; R: recurrence; LQ/UQ: lower/upper quartile; "|": logical operator for "or"; Gray: absorbed dose of ionizing radiation [1 J/kg]; LA: local adjuvant; MM: methyl-methacrylate; BC: bone chips.

2.3. DNA index tested using flow cytometry

The detailed protocol of the DNA content measurement using flow-cytometry was described earlier [58]. In brief, nuclear suspension of trimmed cryopreserved tissue was tested according to a modified Vindelov method [59,60] using BD Cycletest Plus DNA Kit (BD Biosciences, San Jose, CA, USA). Two thousand cell nuclei per surgical case were measured using BD FACS (fluorescence-activated cell sorting) scan and analyzed in the BD CellFit™ software [58]. The DNA distribution of a normal bone marrow was used as a reference. DNA index (DI) was calculated as the ratio of G0/G1 peaks of cell populations in GCTB specimens compared to the reference normal samples [61]. Diploid and poly-/aneuploid cases were defined as $DI = 1$ or $DI \neq 1$, respectively.

2.4. Scoring

Three independent assessors (MEM, KZ, KT) blinded to all clinical- and other cell cycle marker expression data evaluated the

Table 2
Summary of progression events and censored cases.

Type of surgical material[a]	Number of surgical cases	Number of progression events[b] during follow-up	%	Number of cases censored[c]	%
Primary	100	23	23	77	77
1st Recurrence	37	8	21.6	29	78.4
2nd or 3rd Recurrence	16	8	50	8	50
Metastasis	1	1	100	0	0
Total:	154	40	26%	114	74%

[a] Primary: material from first-ever operation; 1.–3. Recurrence(s): patient had previous operation(s) either at IOR or at another institution; metastasis: lung embolus.
[b] Progression events are detailed in Table 3.
[c] Censored: no progression event occurred during follow-up.

Table 3
Specification of progression events occurred during the follow-up.

Disease course during follow-up (FU)	Number of cases	%	Number of progression events	Description of the progression event
Continuously disease-free	114	74	–	no progression event occured
Alive with disease	4	2.6	1	bone metastasis
			3	lung metastasis (embolus)
Death	11	7.1	1	death of other cause (stroke)
			1	death of operation complication
			3	death and lung metastasis
			6	death and transformation to malignant sarcoma with 2–4× recurrences and/or lung metastasis during FU
Local recurrences	25	16.2	17	1× local recurrence during FU
			7	2× local recurrences during FU
			1	2× local recurrences +1 lung metastasis during FU
Total:	154		40[a]	

[a] These progression events provided the basis for progression-free survival analyses using PWP gap-time models.

Table 4
Scoring scheme and the frequency of scores.

Cell cycle marker	Score				
	0 Minimal	1 Low	2 Medium	3 High	N_{sum}
	< 1%	1 ≤ – < 10%	10 ≤ – < 20%	20% ≤	
Ki-67 MIB-1	10	57	71	16	154
	< 1%	1 ≤ – < 10%	10 ≤ – < 20%	20% ≤	
Ki-67 SP6	4	25	97	28	154
	< 5%	5 ≤ – < 20%	20 ≤ – < 40%	40% ≤	
Ki-67 B56	5	19	79	51	154
	< 1%	1 ≤ – < 10%	10 ≤ – < 40%	40% ≤	
Mcm2	7	28	86	33	154
	< 1%	1 ≤ – < 5%	5 ≤ – < 20%	20% ≤	
Cyclin D1	2	66	57	29	154
	< 1%	1 ≤ – < 5%	5 ≤ – < 20%	20% ≤	
Cdk4[a]	2	33	80	38	153
	< 1%	1 ≤ – < 5%	5 ≤ – < 15%	15% ≤	
Cdk2	2	34	67	51	154
	< 5%	5 ≤ – < 10%	10 ≤ – < 20%	20% ≤	
Cyclin A	29	54	55	16	154
	< 3%	3 ≤ – < 10%	10 ≤ – < 20%	20% ≤	
Geminin	6	39	83	26	154
	< 5%	1 ≤ – < 10%	10 ≤ – < 30%	30% ≤	
$p21^{waf1}$	1	20	93	40	154
	Diploid (DI = 1)		Aneuploid (DI ≠ 1)		
Ploidy (DI)	134		20		154

DI: DNA index.
[a] One Cdk4 could not be scored due to slide damage, hence it was left out from all multivariate models which included Cdk4.

immunostained samples ($n = 215$) using whole digital slides (Pannoramic System, 3DHISTECH, Budapest, Hungary). To set appropriate scoring thresholds, each marker was manually scored in a random subset of 20 cases in at least 3 different osteoclast/giant cell rich high power fields (40×) of each 2 mm diameter TMA core. Each reader counted the proportion of the nuclear reactions in biomarker positive mononuclear cells in relation to all mononuclear cells. For each marker, the cut-off results were averaged among readers on a four-grade scale (0 – minimal, 1 – low, 2 – medium, 3 – high proportion) (Table 4). From the 154 surgical cases 215 TMA tissue cores were created including duplicates from 56 cases (112), triplicate from a single case (3) and a single sample from each of the remaining 100 cases. If different scores were given to duplicate or triplicate parallel TMA samples (115/215, 53.5%), always the higher scores were considered for statistical analyses. Samples with discrepant scores among readers were reassessed and consensus scores were agreed on. Cases with incomplete scoring, missing clinicopathological or follow-up data (3/157; 1.9%) were excluded (Table 1).

2.5. Statistical analysis

A stratified Cox-type model, the Prentice-Williams-Peterson gap-time model (PWP-GT) of the SAS 9.4 software were used (SAS Institute Inc., Cary, NC, USA) for time-to-event analyses, which can account for multiple events per patient [62,63]. Biomarker expression marks were dichotomized (negative: scores 0–1 versus positive: scores 2–3) resulting in balanced number of cases within groups (Table 4).

The primary endpoint of the study was PFS defined as follows: recurrence, local- (i.e. bone) or distant metastasis (e.g. lung), malignant transformation (mostly into osteosarcoma), or death of any cause, which made up a total of 40 progression events ($n_{event} = 40$) (Tables 2-3). Following univariate survival analysis with each marker, multivariate testing of all possible combinations up to 5 variables were done using PWP models with the variable selection based on the Akaike Information Criterion (AIC) [64]. AIC is favored in the setting of small number of events for finding optimal number of predictor variables [65]. Clinicopathological factors including age at diagnosis, gender, localization, and treatment type were also considered in multivariate models. Finally, additional interaction models were evaluated to check whether the direction of effects stayed consistent and to uncover possible interactions between cell cycle marker expression levels [66].

We also performed time-to-first-event analyses to check whether the inclusion of multiple events has an influence on the results. Four patients presented incongruent staining results i.e. were concurrently G1-phase negative but post-G1 phase positive. In a sensitivity analysis by repeated testing after discarding these patients we checked if previously proposed models stayed stable. All tests were exploratory and p-values of < 0.05 were considered significant.

The cell cycle profile was characterized with Spearman's rank correlation coefficient based hierarchical clustering using dendrograms (with complete linkage) and heat-maps [67]. This has the advantage of taking into account how the proportions of pre- and post-G1 phase marker positive cell fractions change concurrently instead of just using their absolute distances [68]. For data visualization including Kaplan-Meier survival curves [69] the R statistical environment (v.3.3.3) was used [70].

3. Results

3.1. Study cohort characteristics

The clinicopathological and survival characteristics of the patients are summarized in Tables 1-3. One hundred patients (72%) had primary GCTB, while recurrent tumors made up 28% (39/139) of the cohort. Three quarter of the cases (74%; 114/154) had benign course, whereas progression events occurred in 26% (40/154) of which local recurrences were 62.5% (25/40), 15% (6/40) showed malignant transformation with fatal outcome. Pulmonary metastases (emboli) were

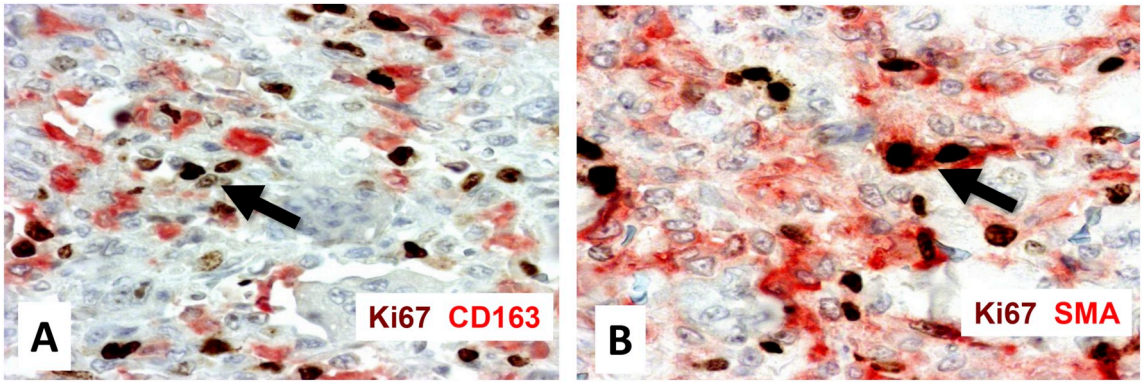

Fig. 1. The majority of the proliferating, Ki67 positive mononuclear cells are CD163 negative (A, arrow), while many of them show smooth muscle actin (SMA) positivity (B, arrow).

found in 13 cases (8.4%) during the entire disease course, and the overall mortality rate was 7.9% (11/139).

3.2. Cell cycle marker detection in GCTB mononuclear cells

All cell cycle markers showed nuclear immunoreaction (except cdk2 and cdk4 which showed some additional cytoplasmic staining) and positive cells were predominantly found in the mononuclear cell fraction of GCTB, except for cyclin D1 and $p21^{waf1}$, which were also detected in multinuclear giant cells. However, only the mononuclear cells were considered at scoring. Most proliferating (Ki-67 positive) mononuclear cells were negative for the macrophage specific scavenger receptor protein CD163 and occasionally α-SMA positive indicating dominantly their stromal cell origin (Fig. 1). Expression of cell cycle markers during phases of cell replication is summarized in Suppl. Table 1.

3.3. Correlation based hierarchical clustering of cell cycle marker expression in GCTB

Hierarchical cluster analysis based on Pearson's correlations showed no major defects of the cell cycle regulation in GCTB (Fig. 2). Cyclin dependent kinases showed the highest correlation with their respective cyclins (cdk2-cyclin A) or inhibitors (cyclin D1-$p21^{waf1}$) and clustered around each other, except for cdk4. Also, the general proliferation marker Ki-67, the replication licensing factor mcm2 and its repressor geminin formed a common subcluster. The extremely few mononuclear cells showing phospho-histone H3 reaction did not allow a systemic comparison and reflected a negligible M-phase cell fractions in this GCTB cohort. This again supported the notion that proliferating cells in GCTB progressed through the cycle without major cell cycle arrest.

3.4. Univariate analysis of cell cycle marker expression for progression-free survival

Univariate survival analysis using PWP-gap time models revealed that poly-/aneuploidy ($p < 0.0001$) against diploid chromosome set and the elevated cyclin A ($p < 0.001$), geminin ($p = 0.015$), mcm2 ($p = 0.016$) and cyclin D1 ($p = 0.022$), positive mononuclear cell fractions had significant negative association with PFS (Fig. 3). Of the Ki67 immunoreactions, B56 ($p = 0.0543$) and Mib1 ($p = 0.0564$) clone positive cell fractions showed also a strong positive trend towards reduced PFS.

3.5. Model selection for cell cycle marker panel-based progression-free survival analysis

3.5.1. Standard multivariate models without interaction

For standard models all possible combinations of cell cycle and clinical markers up to 5 variables were used without testing for possible interactions among them. The AIC-based best multivariate prognostic model (AIC = 271.6) included ploidy (HR = 6.20, 95% CI: 2.89–13.30, $p < 0.0001$), cyclin D1 (HR = 2.27, 95% CI: 1.10–4.71, $p = 0.0274$), mcm2 (HR = 2.64, 95% CI: 0.86–8.08, $p = 0.0901$). The second-best model (AIC = 271.8) additionally involved cyclin A (HR = 1.62, 95% CI: 0.81–3.23, $p = 0.1732$). The third (AIC 272.48) was made up by the same markers as the second but without mcm2, the fourth (AIC 273.18) combined ploidy and cyclin D1 and the fifth was the same as the second where cyclin A was substituted for geminin (AIC 273.30) (Table 5).

All multivariate models used a diploid case which was negative for other markers as a reference (HR = 1) to predict hazard of progression. Detailed analysis of the best multivariate model (including ploidy, mcm2, cyclin D1)-based prediction of PFS showed progressively increasing hazards linked to elevated cell cycle commitment and abnormal chromosome numbers, in support of our modeling (Table 6). For instance, a diploid but mcm2 positive case (i.e. cell cycle entry/initial G1-phase) would show a 163% increased instantaneous hazard of progression (HR = 2.63) compared to the reference. If this hypothetic case was additionally cyclin D1 (G1-S phase transition) positive, the HR would increase to 5.99. If these examples were non-diploid (poly-/aneuploid, DNA index (DI ≠ 1), the predicted HRs would go up to 16.33 and 37.11, respectively.

3.5.2. Interaction models for progression-free survival

We also tested all possible interactions between biomarkers to check whether their association with PFS and the signs of these effects would stay consistent across different expression levels. The highest-ranked interaction model (AIC = 269.5) included ploidy (HR 5.6 8, 95%CI: 2.62–12.31, $p < 0.0001$), mcm2 ($p = 0.609$), cyclin D1 (HR 1.89, 95%CI: 0.88–4.09, $p = 0.105$) and cyclin A ($p < 0.0001$). This is the same as the second best performing standard model with a significant interaction between cyclin A and mcm2 ($p < 0.0001$) where the main effect of cyclin A stayed significant ($p < 0.0001$) and could be interpreted regardless of the interaction.

This model estimated similar HRs to the best standard multivariate models without interaction term and also showed positive correlation between increasing hazards and cell cycle phase progression (see details in Suppl. Table 2). Survival curves of cell cycle phenotypes based on the best interaction model predictions of progression hazard are presented in Fig. 4.

The second-ranked multivariate interaction model (AIC = 273.5) was very similar to this, as it was an extension of the best standard

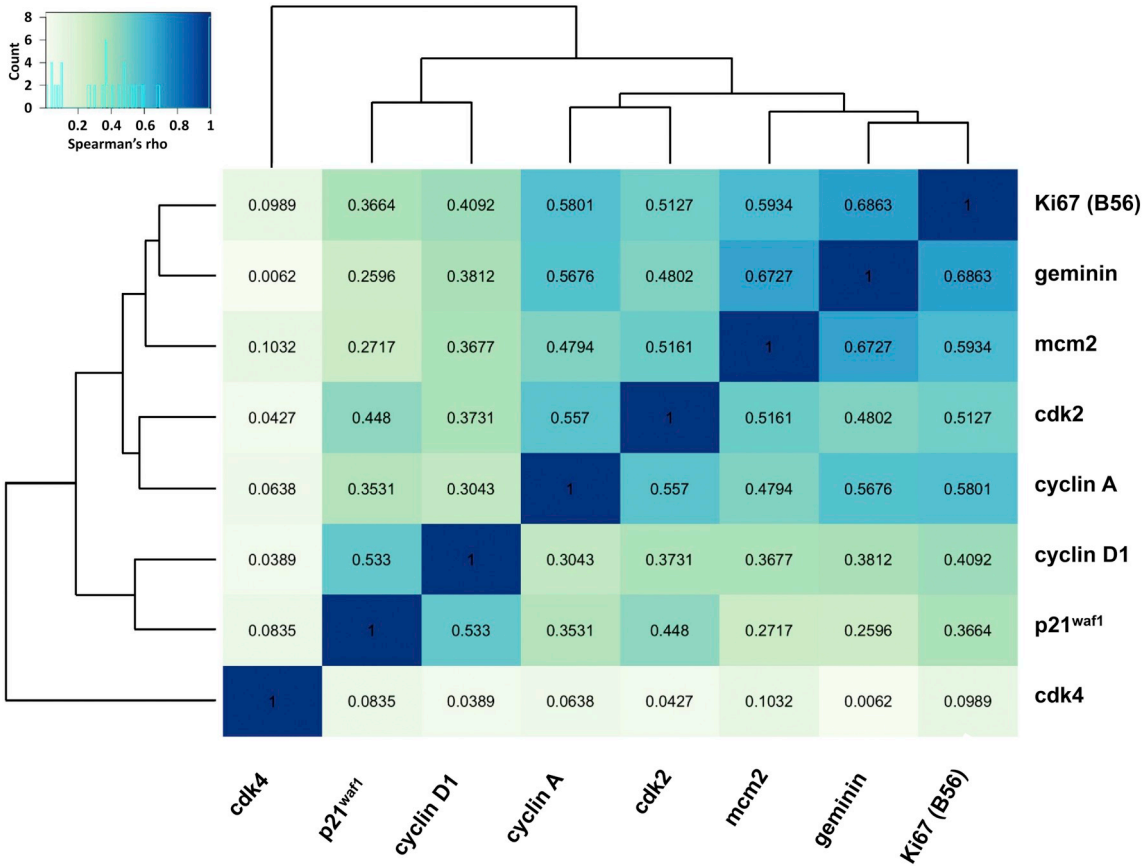

Fig. 2. Heatmap and dendrograms of unsupervised hierarchical clustering of cell cycle marker expression in GCTB mononuclear cells. Spearman's rank correlation coefficients (rho) are seen in the colour scheme (upper-left corner) and as numbers inside boxes. Licensing related enzymes (mcm2-geminin) or cdks and their respective cyclins (cdk2-cyclin A) or inhibitors (cyclin D1-p21^{waf1}) are clustered around each other in line with their regulatory functions in a roughly normal replication cycle.

model (ploidy, mcm2 and cyclin D1) with an additional interaction term between mcm2 and cyclin D1.

3.5.3. Sensitivity analysis of cell cycle based prognostic markers on progression free survival

After excluding those 4 patients with incongruent (post-G1 phase positive, yet licensing negative) staining profiles, we found no relevant interaction regardless of the model building strategy. The top ten ranked models of the sensitivity analyses are presented in Suppl. Table 3. The best-ranked model (AIC = 265.7) consisted of the same markers as the 3rd top standard multivariate model including ploidy (HR = 5.73, 95%CI: 4.74–6.72, $p < 0.0001$); cyclin A:HR = 2.25, 95%CI: 1.22–3.28, $p = 0.0362$; and cyclin D1:HR = 1.93, 95% CI: 0.88–2.97, $p = 0.0977$). The model that additionally included gender/sex ranked 3rd (AIC = 266.91). Combining the best model with clinicopathological factors such as treatment type (rank 4; AIC = 267.01), treatment plus gender (rank 5; AIC = 267.4), or age at first diagnosis (rank 9; AIC = 267.6) only occurred during sensitivity analyses. Models with the addition of Ki-67 clone B56 (AIC = 267.4) and geminin (AIC = 267.5) ranked 6th and 7th respectively.

Similar model to the strongest interaction model, but without any interaction term ranked 8th and contained ploidy (HR 5.68, 95%CI: 4.68–6.68, p < 0.0001), cyclin A (HR 2.07, 95%CI: 1.04–3.10, $p = 0.0839$), cyclin D1 (HR 1.89, 95%CI: 0.86–2.93, $p = 0.1053$) and mcm2 (HR 1.32, 95%CI: 0.42–2.23, $p = 0.609$).

4. Discussion

Despite its rarity and benign behavior GCTB, a locally aggressive osteolytic lesion, can seriously compromise skeletal functions resulting in poor quality of life, severe pain and even fatal consequences [3]. Though GCTB shows high recurrence potential (up to 75%, depending on treatment regimens) [3], occasional malignant transformation (up to 10%) and pulmonary metastases (up to 7%) [71], its clinical progression is still insufficiently understood and can be inaccurately predicted [3,14,73]. Cell cycle integrates the effects of both the dysregulated replication control and upstream growth signaling pathways, therefore, elevated cell cycle progression is usually linked with less favorable outcome of tumor evolution [13]. Accordingly, we performed an in situ cell cycle analysis in a large cohort of 154 surgical GCTB cases from 139 patients using DNA flow cytometry and immunohistochemistry. Our comprehensive marker testing revealed that GCTB patients with elevated post-G1 phase mononuclear cell fractions had significantly increased risk for reduced PFS.

Detection of aberrant and accelerated cell cycle progression has emerged as a powerful diagnostic and prognostic tool in many tumor types [28,45]. Though H3F3A G34W mutant neoplastic stromal cells show elevated proliferation in culture [72], this genetic aberration affects the vast majority (90–95%) of GCTB cases. Therefore, it is likely that diverse proliferation rates among cases may result from the differences in the proportions of H3F3A G34W neoplastic stromal cells, in telomere associations [18], in the activation of upstream growth signaling, e.g. through EGFR, c-Met or Wnt pathways [8,73,74], or in deregulated Cx43 cell-communication [10]. Spearman's rank correlation-based clustering [68] of cell cycle marker expression in our GCTB cohort revealed close association between replication licensing (mcm2) and cyclin-dependent kinases, and between cdk-s and their respective cyclins or inhibitors. This implied no major cell cycle arrested fractions

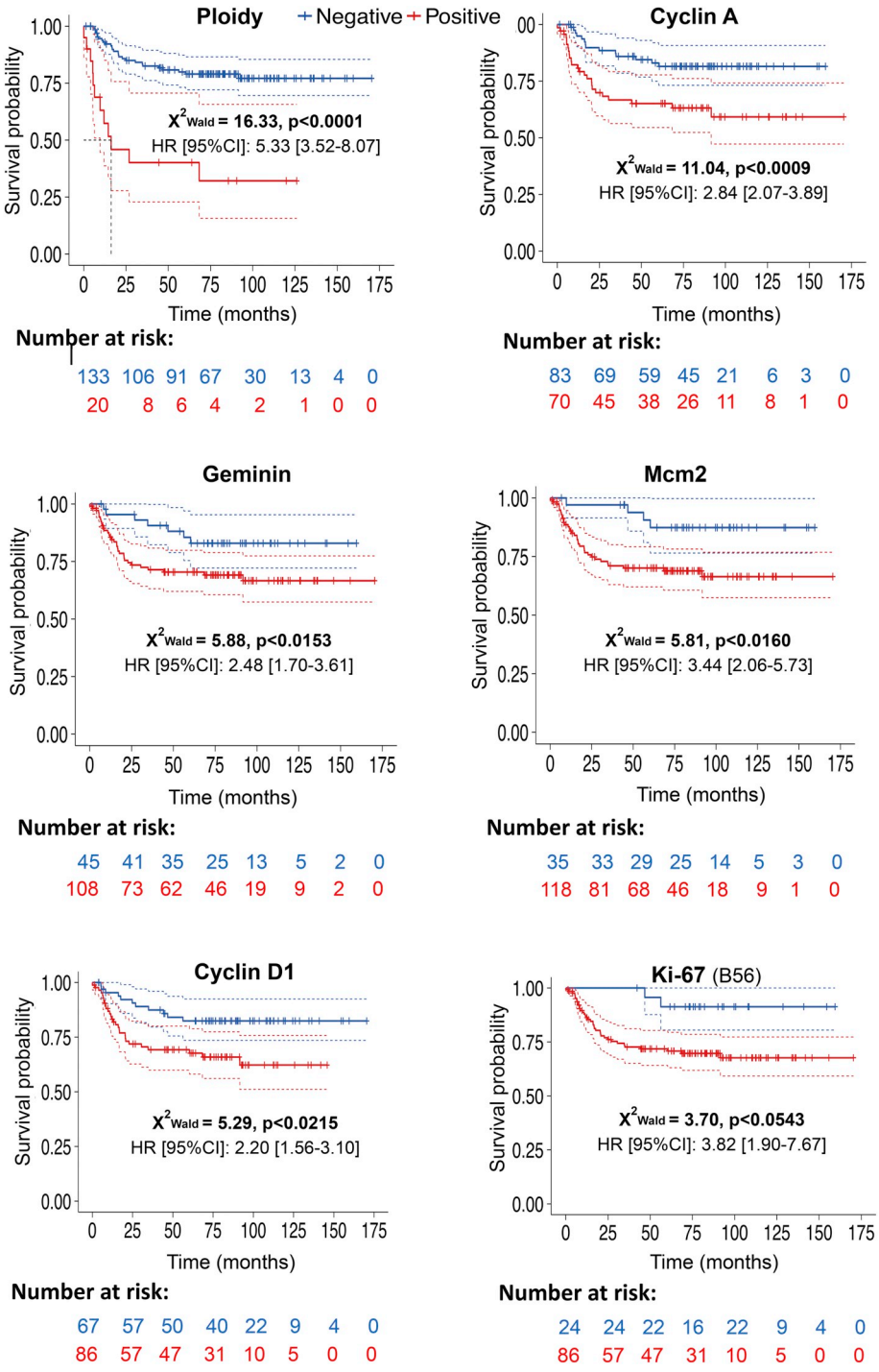

Fig. 3. Time-to-event (n = 153) Kaplan-Meier plots of cell cycle marker expression with the strongest univariate association with PFS using PWP gap-time models. Expression levels were dichotomized along median scores, negative (blue) vs. positive (red). Hazard ratios (HR) are shown including 95% confidence interval (CI, dashed lines), censoring is marked by "+". (For interpretation of the references to colour in this figure legend, the reader is referred to the web version of this article.)

in GCTB mononuclear cells [32].

The proliferating, Ki67 positive cell fraction (covering the whole cycle), as we showed here with double immunolabeling, was dominated by neoplastic stromal cells. Earlier studies of cell proliferation and GCTB progression have used only a limited selection of individual markers mostly testing only relatively low number of cases. These suggested that increased frequency of the general proliferation marker Ki-67 (Mib1 clone) [12], the G1-phase indicator cyclin D1 and cyclin D3 [51], the G2/M-phase promoter cyclin B1 [52] and the cdk4/6 inhibitor $p21^{waf1}$ [53] positive cells can show significant positive correlation with GCTB recurrence and aggressive behavior. A recent work in a large tumor cohort (n = 164) revealed that besides the femoral and humeral localization, elevated number of cyclin D1 positive giant cells were associated with GCTB relapses [54]. Though this study used multivariate logistic regression with recurrence as a binary endpoint it did not consider repeated events of individual patients as opposed to our PWP-GT models. Therefore, earlier studies have neither informed about the kinetics of the cell cycle, nor have modeled the disease course with multiple recurring events.

Our univariate PWP-GT models showed ploidy (poly-/aneuploid vs

Table 5
Top 10 multivariate PWP-models using AIC based model selection.

Rank	Model description	Criteria	Value
1	Ploidy + Mcm2 + Cyclin D1	AIC	271.56
2	Ploidy + Mcm2 + Cyclin D1 + Cyclin A	AIC	271.84
3	Ploidy + Cyclin D1 + Cyclin A	AIC	272.48
4	Ploidy + Cyclin D1	AIC	273.18
5	Ploidy + Mcm2 + Cyclin D1 + Geminin	AIC	273.30
6	Ploidy + Mcm2 + Cyclin D1 + Ki-67 B56	AIC	273.36
7	Ploidy + Mcm2 + Cyclin D1 + Ki-67 Mib1	AIC	273.38
8	Ploidy + Mcm2 + Cyclin D1 + Cdk2	AIC	273.41
9	Ploidy + Mcm2 + Cyclin D1 + Gender/Sex	AIC	273.41
10	Ploidy + Mcm2 + Cyclin D1 + $p21^{waf1}$	AIC	273.42

Table 6
Best multivariate model-based prediction of progression-free survival (PFS).

Ploidy	Mcm2	Cyclin D1	Hazard ratio (HR)
Diploid	neg.	neg.	Reference = 1
Diploid	neg.	pos.	2.27
Diploid	pos.	neg.	2.63
Diploid	pos.	pos.	5.99
Aneuploid	neg.	neg.	6.19
Aneuploid	neg.	pos.	14.09
Aneuploid	pos.	neg.	16.33
Aneuploid	pos.	pos.	37.11

diploid cases) and the expression in the mononuclear cell fraction of cyclin-A and geminin as the strongest negative predictors of PFS followed by mcm2 and cyclin D1. This was consistent with an accelerated cell cycle progression in the tumors of less favorable outcome in line with published results e.g. in breast and renal cell carcinomas and in melanomas [27,75,76]. These results were also in line with our cluster analysis, where licensing related mcm2 levels showed higher correlation with those of the S-G2-M promoter cyclin A and the late cell cycle repressor geminin [47,77] than with the G1-S phase catalyzers cyclin D1 and cdk4 [14,76]. Positive cell fractions with B56 ($p = 0.0543$) and Mib1 ($p = 0.0564$) clones recognizing Ki67 protein also showed a strong trend towards reduced PFS. These findings confirmed that there was no major cell cycle arrested mononuclear cell population in our GCTB series. Also, they may explain the inconsistent published results of Ki67 detection in GCTB progression, which could be tilted onto either side of the statistical conclusion depending on the representation of this population in the chosen cohort [12,52,54,74].

Our multivariate PWP-GT models that considered the joint effect of multiple markers, also reinforced the pivotal role of ploidy along with cyclin D1, mcm2 and cyclin A as the best panel members for predicting PFS by offering the lowest AIC value. Earlier, we and other groups published evidence on the chromosomal instability of GCTB stromal cells including telomere associations, polysomies and individual-cell aneusomies in association with tumor progression [9,10,16,17,78]. In line with this and as an indicator of genomic instability, ploidy showed the statistically most significant association with reduced PFS in all models in the present study either with or without interaction including the sensitivity analysis.

Of the G1-S-phase transition markers, our study is the first to focus on cyclin D1 expression in GCTB mononuclear cells, which showed invers statistical correlation with PFS as opposed to its complexing partner cdk4/6 [14]. This imbalance suggested additional roles for cyclin D1 to retinoblastoma phosphorylation [53] in neoplastic stromal cells, which might involve components of osteoclastogenesis. Indeed, a study of 32 GCTB cases disclosed widespread expression of both cyclin D1 and cyclin D3 in giant cells and suggested a potential link between this and GCTB pathogenesis but without testing mononuclear cells and finding any correlation with tumor progression [52]. Concerning cyclin D1 expression in giant cells, these findings were in agreement with another work, which however tested only 16 cases (primary and recurrent) altogether [51]. Mononuclear cell cyclin D1 expression in

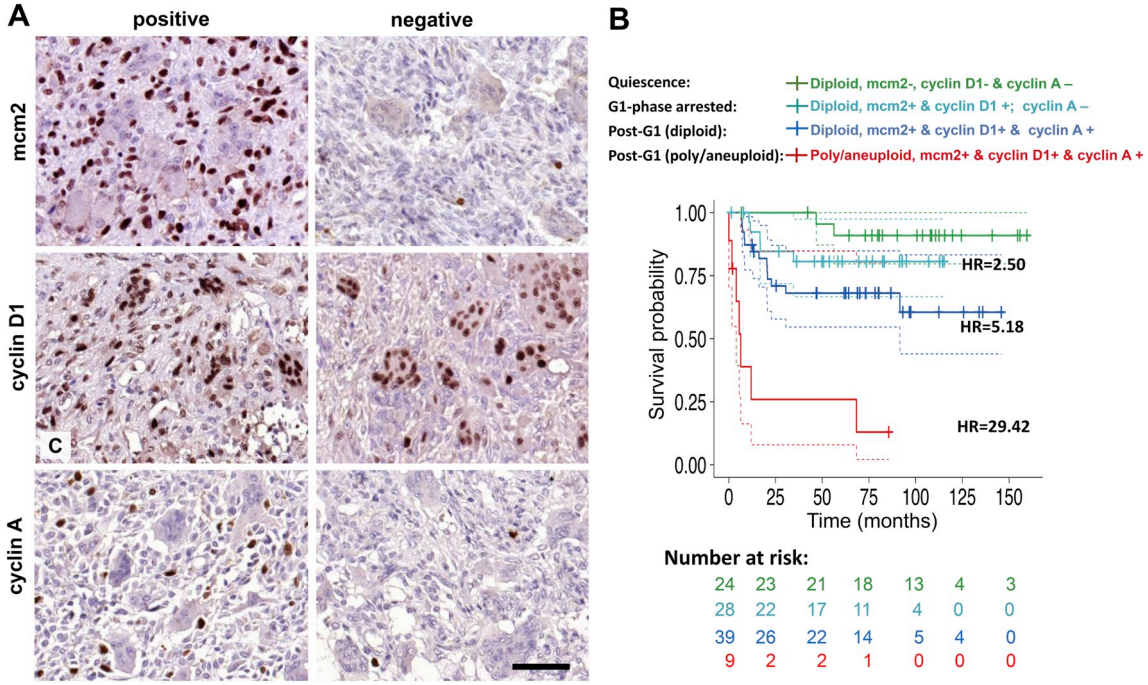

Fig. 4. Representative images of the most significant nuclear cell cycle marker immunoreactions in positive and negative GCTB cases (A; DAB, brown; hematoxylin counterstain blue). Scale bar: 50 µm. Kaplan-Meier curves showing PFS risk groups based on differential marker expression in the mononuclear cell fractions (B). Quiescent (diploid, mcm2, cyclin D1 and cyclin A negative) cases (green) were compared to diploid mcm2, cyclin D1 positive and cyclin A negative G1-phase arrested cases (light blue, HR = 2.50); to diploid post-G1-phase, cyclin A positive cases (dark blue; HR = 5.18); and to poly-/aneuploid post-G1-phase cases (red, HR = 29.42). Reported hazard ratios are based on the best multivariate interaction model (for details see Suppl. Table 2). (For interpretation of the references to colour in this figure legend, the reader is referred to the web version of this article.)

GCTB occurred in all of our top 10 multivariate tests and 9 of the top 10 models in the sensitivity analysis. Its negative correlation with PFS stayed robust even after adjusting for the effect of ploidy and mcm2.

The expression of cyclin A, a post-G1-phase marker, was tested for the first time also by us in GCTB and found in the second-best multivariate immune panel. The complex of cyclin A and cdk2 promotes S-phase and DNA synthesis and also controls the initiation of mitosis through activating the cyclin B1-cdk1 complex and orchestrating their centrosomal and nuclear functions [79]. Though, neither mcm2 nor cyclin A showed individual significance in standard multivariate models after adjusting for the effects of other markers, they could significantly improve the overall model performance and robustness in terms of AIC values, which is probably due to the better coverage of the cell cycle with their inclusion [80,81].

All these results were further verified when we tested for interactions between biomarkers and their association with PFS and see if their influence stays consistent across different expression levels. Accordingly, the most robust multivariate interaction model was the same as the best standard model added with cyclin A of a highly significant main effect and its major interaction with mcm2 (both $p < 0.0001$). Emergence of cyclin A in the panel allowed both the reliable identification of the post-G1 (S-G2-M) phase cell fractions and the G1-phase arrested (mcm2 and cyclin D1 positive but cyclin A negative) cases. Therefore, the results of multivariate analyses both with or without interaction revealed a positive correlation between increasing hazards and cell cycle phase progression consistent with reduced AIC scores when cyclin A was included. The central role of cyclin A in DNA synthesis and S-G2-M phase was emphasized by its presence in all the top 10 models of sensitivity analysis. Similar findings were published in high grade osteosarcoma where patients with cyclin A overexpression showed elevated risk for relapsing [82] and in melanoma where increased cyclin A positive post-G1-phase cell fractions differentiated them from dysplastic nevi [27].

Geminin, also an indicator of G2-M-phase cells, has been reported too as a marker of tumor progression and adverse prognosis in colon [83] and breast cancers [84], as well as in high-grade astrocytomas [85]. In our study it served as a somewhat less prominent alternative of cyclin A by occurring in the 5th best performing model of the whole dataset and in the second highest ranked extended model, based solely on cell cycle markers, during the sensitivity analysis. Notably, most geminin positive cases were also cyclin A positive in our independent blinded scoring. Therefore, it can also be a candidate for prognostic modeling of GCTB similarly to those results published in renal cell and breast carcinomas [75,76].

Interestingly, clinical variables emerged only during the sensitivity analysis as non-significant but still relevant predictors. The effect of surgical treatment on PFS was less critical compared to those of the cell cycle markers. Gender/sex occurred only in the top 3rd model, surgical treatment was seen in the 4th, treatment combined with gender in the 5th, and age at diagnosis in the 9th ranked model (see Table 8). Though treatment was a non-significant predictor in our cohort, it could improve model performance. In a large cohort study of Chinese GCTB patients using uni- and multivariate Cox-proportional hazard analyses showed that local recurrence rates after curettage was accompanied by significantly higher frequency of recurrences than after using the more invasive wide resection [86]. Additionally, they found shorter recurrence free periods for younger (< 30 yrs) versus older (> 30 yrs) patients but, somewhat contrasting to our analysis, no relevant gender effect.

Optimizing cell cycle related antibodies by careful preselection and setting up their reliable detection in formalin-fixed paraffin-embedded sections, as well as by using pretested antigen retrieval conditions and highly sensitive detection polymer system, were key factors for reliable and reproducible immunoreaction and analysis in this and our earlier study [27]. The feasibility of this approach is supported by the fact that despite blinded scoring, implausible staining (post-G1 phase positive, yet licensing negative) results occurred only in four cases (2.6%). As a result, this is the first study of utilizing a comprehensive cell cycle-based phenotyping of GCTB statistically tested with the most appropriate AIC-based PWP survival modeling, which account for multiple recurrences during the course of the disease [63].

5. Conclusions

In conclusion, ploidy and in situ detection of a subset of distinct cell cycle phase indicators including the replication licensing mcm2, the G1-phase cyclin D1 and the S-G2-M phase cyclin A can cover key regulatory elements of cell replication and allow relevant survival phenotyping of GCTB cases. Detecting this restricted panel of antigens using immunocytochemistry and of ploidy with flow cytometry at reasonable costs are available in centers of soft tissue pathology. This approach can be exploited for identifying GCTB patients with higher risk of recurrence where more careful follow up and/or adjuvant RANKL inhibitor or bisphosphonate treatment may additionally be required.

Author contributions

Conceived and designed the experiments: TK. Performed the experiments: MEM, ZK, BP and PP. Analyzed the data: SS, MEM, TK and PP. Contributed reagents/materials/analysis tools: MSB, PP, ZS and LT. Diagnosing GCTB cases and advising on the study: MSz, ZS and RF. Writing original draft: MEM and SS. Supervising experiments and writing, review & editing final manuscript: TK.

Funding

This study was supported by EuroBoNet, an EU FP6 granted Network of Excellence Program (LSHC-CT-2006-018814) and by a grant (NVKP_16-1-2016-0004) from the Hungarian National Research, Development and Innovation Office (NKFIH). The founders had no influence on study design, data collection, analysis and decision to publish, or prepare the manuscript.

Declaration of Competing Interest

The authors declare no conflict of interests.

Acknowledgements

The authors are grateful to Maria-Serena Benassi for careful case selection and patients' data management, Edit Parsch, Eva Balogh Martaine, for excellent technical assistance and to Laszlo Kopper, Gergo Kiszner, Ivett Teleki and Nora Meggyeshazi for valuable advice.

Appendix A. Supplementary data

Supplementary data to this article can be found online at https://doi.org/10.1016/j.bone.2019.06.022.

References

[1] R.E. Turcotte, J.S. Wunder, M.H. Isler, R.S. Bell, N. Schachar, B.A. Masri, G. Moreau, A.M. Davis, Giant cell tumor of long bone: a Canadian Sarcoma Group study, Clin. Orthop. Relat. Res. 397 (2002) 248–258.
[2] A. Liede, R.K. Hernandez, E.-T. Tang, C. Li, B. Bennett, S.S. Wong, D. Jandial, Epidemiology of benign giant cell tumor of bone in the Chinese population, Journal of bone oncology 12 (2018) 96–100.
[3] J.M. Amelio, J. Rockberg, R.K. Hernandez, P. Sobocki, S. Stryker, B.A. Bach, J. Engellau, A. Liede, Population-based study of giant cell tumor of bone in Sweden (1983-2011), Cancer Epidemiol. 42 (2016) 82–89.
[4] M. Szendröi, Giant-cell tumour of bone, J Bone Joint Surg Br 86 (1) (2004) 5–12.
[5] F. Bertoni, D. Present, A. Sudanese, N. Baldini, P. Bacchini, M. Campanacci, Giant-cell tumor of bone with pulmonary metastases. Six case reports and a review of the

literature, Clin Orthop Relat Res (237) (1988) 275–285.
[6] M.G. Rock, D.J. Pritchard, K.K. Unni, Metastases from histologically benign giant-cell tumor of bone, J. Bone Joint Surg. Am. 66 (2) (1984) 269–274.
[7] M. Balke, H. Ahrens, A. Streitbuerger, G. Koehler, W. Winkelmann, G. Gosheger, J. Hardes, Treatment options for recurrent giant cell tumors of bone, J. Cancer Res. Clin. Oncol. 135 (1) (2009) 149–158.
[8] P. Balla, L. Moskovszky, Z. Sapi, R. Forsyth, H. Knowles, N.A. Athanasou, M. Szendroi, L. Kopper, H. Rajnai, F. Pinter, I. Petak, M.S. Benassi, P. Picci, A. Conti, T. Krenacs, Epidermal growth factor receptor signalling contributes to osteoblastic stromal cell proliferation, osteoclastogenesis and disease progression in giant cell tumour of bone, Histopathology 59 (3) (2011) 376–389.
[9] L. Moskovszky, K. Dezso, N. Athanasou, M. Szendroi, L. Kopper, K. Kliskey, P. Picci, Z. Sapi, Centrosome abnormalities in giant cell tumour of bone: possible association with chromosomal instability, Mod. Pathol. 23 (3) (2010) 359–366.
[10] P. Balla, M.E. Maros, G. Barna, I. Antal, G. Papp, Z. Sapi, N.A. Athanasou, M.S. Benassi, P. Picci, T. Krenacs, Prognostic impact of reduced connexin43 expression and gap junction coupling of neoplastic stromal cells in giant cell tumor of bone, PLoS One 10 (5) (2015) e0125316.
[11] H.J. Knowles, N.A. Athanasou, Canonical and non-canonical pathways of osteoclast formation, Histol. Histopathol. 24 (3) (2009) 337–346.
[12] I. Antal, Z. Sapi, M. Szendroi, The prognostic significance of DNA cytophotometry and proliferation index (Ki-67) in giant cell tumors of bone, Int. Orthop. 23 (6) (1999) 315–319.
[13] S. Behjati, P.S. Tarpey, N. Presneau, S. Scheipl, N. Pillay, P. Van Loo, D.C. Wedge, S.L. Cooke, G. Gundem, H. Davies, S. Nik-Zainal, S. Martin, S. McLaren, V. Goody, B. Robinson, A. Butler, J.W. Teague, D. Halai, B. Khatri, O. Myklebost, D. Baumhoer, G. Jundt, R. Hamoudi, R. Tirabosco, M.F. Amary, P.A. Futreal, M.R. Stratton, P.J. Campbell, A.M. Flanagan, Distinct H3F3A and H3F3B driver mutations define chondroblastoma and giant cell tumor of bone, Nat. Genet. 45 (12) (2013) 1479–1482.
[14] G.H. Williams, K. Stoeber, The cell cycle and cancer, J. Pathol. 226 (2) (2012) 352–364.
[15] M. Wulling, C. Engels, N. Jesse, M. Werner, G. Delling, E. Kaiser, The nature of giant cell tumor of bone, J. Cancer Res. Clin. Oncol. 127 (8) (2001) 467–474.
[16] R.W. Cowan, G. Singh, Giant cell tumor of bone: a basic science perspective, Bone 52 (1) (2013) 238–246.
[17] L. Moskovszky, K. Szuhai, T. Krenacs, P.C. Hogendoorn, M. Szendroi, M.S. Benassi, L. Kopper, T. Fule, Z. Sapi, Genomic instability in giant cell tumor of bone. A study of 52 cases using DNA ploidy, relocalization FISH, and array-CGH analysis, Genes Chromosomes Cancer 48 (6) (2009) 468–479.
[18] G. De Boeck, R.G. Forsyth, M. Praet, P.C. Hogendoorn, Telomere-associated proteins: cross-talk between telomere maintenance and telomere-lengthening mechanisms, The Journal of Pathology: A Journal of the Pathological Society of Great Britain and Ireland 217 (3) (2009) 327–344.
[19] N. Presneau, D. Baumhoer, S. Behjati, N. Pillay, P. Tarpey, P.J. Campbell, G. Jundt, R. Hamoudi, D.C. Wedge, P.V. Loo, A.B. Hassan, B. Khatri, H. Ye, R. Tirabosco, M.F. Amary, A.M. Flanagan, Diagnostic value of H3F3A mutations in giant cell tumour of bone compared to osteoclast-rich mimics, J Pathol Clin Res 1 (2) (2015) 113–123.
[20] F. Amary, F. Berisha, H. Ye, M. Gupta, A. Gutteridge, D. Baumhoer, R. Gibbons, R. Tirabosco, P. O'Donnell, A.M. Flanagan, H3F3A (histone 3.3) G34W immunohistochemistry: a reliable marker defining benign and malignant Giant cell tumor of bone, Am. J. Surg. Pathol. 41 (8) (2017) 1059–1068.
[21] M. Salerno, S. Avnet, M. Alberghini, A. Giunti, N. Baldini, Histogenetic characterization of giant cell tumor of bone, Clin. Orthop. Relat. Res. 466 (9) (2008) 2081–2091.
[22] M. Werner, Giant cell tumour of bone: morphological, biological and histogenetical aspects, Int. Orthop. 30 (6) (2006) 484–489.
[23] A. Shetty, M. Loddo, T. Fanshawe, A.T. Prevost, R. Sainsbury, G.H. Williams, K. Stoeber, DNA replication licensing and cell cycle kinetics of normal and neoplastic breast, Br. J. Cancer 93 (11) (2005) 1295–1300.
[24] A. Hanna-Morris, S. Badvie, P. Cohen, T. McCullough, H.J.N. Andreyev, T.G. Allen-Mersh, Minichromosome maintenance protein 2 (MCM2) is a stronger discriminator of increased proliferation in mucosa adjacent to colorectal cancer than Ki-67, J. Clin. Pathol. 62 (4) (2008) 325–330.
[25] J. Papay, T. Krenacs, J. Moldvay, E. Stelkovics, J. Furak, B. Molnar, L. Kopper, Immunophenotypic profiling of nonsmall cell lung cancer progression using the tissue microarray approach, Appl. Immunohistochem. Mol. Morphol. 15 (1) (2007) 19–30.
[26] T. De Meyer, I.T. Bijsmans, K.K. Van de Vijver, S. Bekaert, J. Oosting, W. Van Criekinge, M. van Engeland, N.L. Sieben, E2Fs mediate a fundamental cell-cycle deregulation in high-grade serous ovarian carcinomas, J. Pathol. 217 (1) (2009) 14–20.
[27] G. Kiszner, B. Wichmann, I.B. Nemeth, E. Varga, N. Meggyeshazi, I. Teleki, P. Balla, M.E. Maros, K. Penksza, T. Krenacs, Cell cycle analysis can differentiate thin melanomas from dysplastic nevi and reveals accelerated replication in thick melanomas, Virchows Arch. 464 (5) (2014) 603–612.
[28] J.A. Lopez-Guerrero, I. Machado, K. Scotlandi, R. Noguera, A. Pellin, S. Navarro, M. Serra, S. Calabuig-Farinas, P. Picci, A. Llombart-Bosch, Clinicopathological significance of cell cycle regulation markers in a large series of genetically confirmed Ewing's sarcoma family of tumors, Int. J. Cancer 128 (5) (2011) 1139–1150.
[29] K. Vermeulen, D.R. Van Bockstaele, Z.N. Berneman, The cell cycle: a review of regulation, deregulation and therapeutic targets in cancer, Cell Prolif. 36 (3) (2003) 131–149.
[30] G.H. Williams, K. Stoeber, Cell cycle markers in clinical oncology, Curr. Opin. Cell Biol. 19 (6) (2007) 672–679.
[31] M.D. Planas-Silva, R.A. Weinberg, The restriction point and control of cell proliferation, Curr. Opin. Cell Biol. 9 (6) (1997) 768–772.
[32] A. Zetterberg, O. Larsson, Kinetic analysis of regulatory events in G1 leading to proliferation or quiescence of Swiss 3T3 cells, Proc. Natl. Acad. Sci. U. S. A. 82 (16) (1985) 5365–5369.
[33] K. Stoeber, T.D. Tlsty, L. Happerfield, G.A. Thomas, S. Romanov, L. Bobrow, E.D. Williams, G.H. Williams, DNA replication licensing and human cell proliferation, J. Cell Sci. 114 (Pt 11) (2001) 2027–2041.
[34] M.A. Gonzalez, K.K. Tachibana, R.A. Laskey, N. Coleman, Innovation - control of DNA replication and its potential clinical exploitation, Nat. Rev. Cancer 5 (2) (2005) 135–141.
[35] J.J. Blow, A. Dutta, Preventing re-replication of chromosomal DNA, Nat Rev Mol Cell Biol 6 (6) (2005) 476–486.
[36] S.R. Kingsbury, M. Loddo, T. Fanshawe, E.C. Obermann, A.T. Prevost, K. Stoeber, G.H. Williams, Repression of DNA replication licensing in quiescence is independent of geminin and may define the cell cycle state of progenitor cells, Exp. Cell Res. 309 (1) (2005) 56–67.
[37] T. Scholzen, J. Gerdes, The Ki-67 protein: from the known and the unknown, J. Cell. Physiol. 182 (3) (2000) 311–322.
[38] K.W. Orford, D.T. Scadden, Deconstructing stem cell self-renewal: genetic insights into cell-cycle regulation, Nat Rev Genet 9 (2) (2008) 115–128.
[39] J.W. Harbour, R.X. Luo, A. Dei Santi, A.A. Postigo, D.C. Dean, Cdk phosphorylation triggers sequential intramolecular interactions that progressively block Rb functions as cells move through G1, Cell 98 (6) (1999) 859–869.
[40] J. Bartek, J. Bartkova, J. Lukas, The retinoblastoma protein pathway and the restriction point, Curr. Opin. Cell Biol. 8 (6) (1996) 805–814.
[41] C.J. Sherr, J.M. Roberts, Inhibitors of mammalian G1 cyclin-dependent kinases, Genes Dev. 9 (10) (1995) 1149–1163.
[42] A. Carnero, G.J. Hannon, The INK4 family of CDK inhibitors, Curr. Top. Microbiol. Immunol. 227 (1998) 43–55.
[43] J.W. Harper, S.J. Elledge, K. Keyomarsi, B. Dynlacht, L.H. Tsai, P. Zhang, S. Dobrowolski, C. Bai, L. Connell-Crowley, E. Swindell, et al., Inhibition of cyclin-dependent kinases by p21, Mol. Biol. Cell 6 (4) (1995) 387–400.
[44] M. Arellano, S. Moreno, Regulation of CDK/cyclin complexes during the cell cycle, Int. J. Biochem. Cell Biol. 29 (4) (1997) 559–573.
[45] A.W. Murray, Recycling the cell cycle: cyclins revisited, Cell 116 (2) (2004) 221–234.
[46] K.E. Tachibana, M.A. Gonzalez, N. Coleman, Cell-cycle-dependent regulation of DNA replication and its relevance to cancer pathology, J. Pathol. 205 (2) (2005) 123–129.
[47] G. Xouri, A. Squire, M. Dimaki, B. Geverts, P.J. Verveer, S. Taraviras, H. Nishitani, A.B. Houtsmuller, P.I. Bastiaens, Z. Lygerou, Cdt1 associates dynamically with chromatin throughout G1 and recruits geminin onto chromatin, EMBO J. 26 (5) (2007) 1303–1314.
[48] C.J. Sherr, J.M. Roberts, Living with or without cyclins and cyclin-dependent kinases, Genes Dev. 18 (22) (2004) 2699–2711.
[49] B. Lacroix, A.S. Maddox, Cytokinesis, ploidy and aneuploidy, J. Pathol. 226 (2) (2012) 338–351.
[50] N.J. Ganem, D. Pellman, Limiting the proliferation of polyploid cells, Cell 131 (3) (2007) 437–440.
[51] S. Matsubayashi, M. Nakashima, K. Kumagai, M. Egashira, Y. Naruke, H. Kondo, T. Hayashi, H. Shindo, Immunohistochemical analyses of β-catenin and cyclin D1 expression in giant cell tumor of bone (GCTB): a possible role of Wnt pathway in GCTB tumorigenesis, Pathology - Research and Practice 205 (9) (2009) 626–633.
[52] A. Kauzman, S.Q. Li, G. Bradley, R.S. Bell, J.S. Wunder, R. Kandel, Cyclin alterations in giant cell tumor of bone, Mod. Pathol. 16 (3) (2003) 210–218.
[53] R. Kandel, S.Q. Li, R. Bell, J. Wunder, P. Ferguson, A. Kauzman, J.A. Diehl, J. Werier, Cyclin D1 and p21 is elevated in the giant cells of giant cell tumors, J. Orthop. Res. 24 (3) (2006) 428–437.
[54] N. Lujic, J. Sopta, R. Kovacevic, V. Stevanovic, R. Davidovic, Recurrence of giant cell tumour of bone: role of p53, cyclin D1, beta-catenin and Ki67, Int. Orthop. 40 (11) (2016) 2393–2399.
[55] W.F. Enneking, A system of staging musculoskeletal neoplasms, Clin Orthop Relat Res (204) (1986) 9–24.
[56] M. Campanacci, N. Baldini, S. Boriani, A. Sudanese, Giant-cell tumor of bone, J. Bone Joint Surg. Am. 69 (1) (1987) 106–114.
[57] T. Krenacs, G. Kiszner, E. Stelkovics, P. Balla, I. Teleki, I. Nemeth, E. Varga, I. Korom, T. Barbai, V. Plotar, J. Timar, E. Raso, Collagen XVII is expressed in malignant but not in benign melanocytic tumors and it can mediate antibody induced melanoma apoptosis, Histochem. Cell Biol. 138 (4) (2012) 653–667.
[58] L. Pazzaglia, M.S. Benassi, P. Ragazzini, G. Gamberi, F. Ponticelli, A. Chiechi, C.M. Hattinger, L. Morandi, M. Alberghini, L. Zanella, P. Picci, M. Mercuri, Molecular alterations of monophasic synovial sarcoma: loss of chromosome 3p does not alter RASSF1 and MLH1 transcriptional activity, Histol. Histopathol. 21 (2) (2006) 187–195.
[59] L.L. Vindelov, I.J. Christensen, A review of techniques and results obtained in one laboratory by an integrated system of methods designed for routine clinical flow cytometric DNA analysis, Cytometry 11 (7) (1990) 753–770.
[60] S.A. Engelholm, M. Spang-Thomsen, L.L. Vindelov, N.A. Brunner, Chemosensitivity of human small cell carcinoma of the lung detected by flow cytometric DNA analysis of drug-induced cell cycle perturbations in vitro, Cytometry 7 (3) (1986) 243–250.
[61] R. Nunez, DNA measurement and cell cycle analysis by flow cytometry, Curr Issues Mol Biol 3 (3) (2001) 67–70.
[62] R.L. Prentice, Relative risk regression analysis of epidemiologic data, Environ. Health Perspect. 63 (1985) 225–234.

[63] R.L. Prentice, B.J. Williams, A.V. Peterson, On the regression-analysis of multivariate failure time data, Biometrika 68 (2) (1981) 373–379.
[64] H. Akaike, Maximum likelihood identification of Gaussian autoregressive moving average models, Biometrika 60 (2) (1973) 255–265.
[65] H.C. van Houwelingen, From model building to validation and back: a plea for robustness, Stat. Med. 33 (30) (2014) 5223–5238.
[66] M. Bradburn, T. Clark, S. Love, D. Altman, Survival analysis part III: multivariate data analysis–choosing a model and assessing its adequacy and fit, Br. J. Cancer 89 (4) (2003) 605–611.
[67] B.B. Gregory, R. Warnes, Lodewijk Bonebakker, Robert Gentleman, Wolfgang Huber Andy Liaw, Thomas Lumley, Martin Maechler, Arni Magnusson, Steffen Moeller, Marc Schwartz, Bill Venables, gplots: Various R Programming Tools for Plotting Data. R Package Version 3.0.1, (2016).
[68] G. James, D. Witten, T. Hastie, R. Tibshirani, An Introduction to Statistical Learning, Springer, New York, 2013.
[69] A. Kassambara, M. Kosinski, P. Biecek, Survminer: Drawing Survival Curves Using ggplot2, R Package Version 0.3 1, (2017).
[70] R Core Team, R, A Language and Environment for Statistical Computing, R Foundation for Statistical Computing, 2016.
[71] L. van der Heijden, P.D.S. Dijkstra, J.-Y. Blay, H. Gelderblom, Giant cell tumour of bone in the denosumab era, Eur. J. Cancer 77 (2017) 75–83.
[72] J. Lim, J.H. Park, A. Baude, Y. Yoo, Y.K. Lee, C.R. Schmidt, J.B. Park, J. Fellenberg, J. Zustin, F. Haller, I. Krucken, H.G. Kang, Y.J. Park, C. Plass, A.M. Lindroth, The histone variant H3.3 G34W substitution in giant cell tumor of the bone link chromatin and RNA processing, Sci. Rep. 7 (1) (2017) 13459.
[73] L. Liu, E. Aleksandrowicz, P. Fan, F. Schönsiegel, Y. Zhang, H. Sähr, J. Gladkich, J. Mattern, D. Depeweg, B. Lehner, Enrichment of c-Met+ tumorigenic stromal cells of giant cell tumor of bone and targeting by cabozantinib, Cell Death Dis. 5 (10) (2014) e1471.
[74] S. Matsubayashi, M. Nakashima, K. Kumagai, M. Egashira, Y. Naruke, H. Kondo, T. Hayashi, H. Shindo, Immunohistochemical analyses of beta-catenin and cyclin D1 expression in giant cell tumor of bone (GCTB): a possible role of Wnt pathway in GCTB tumorigenesis, Pathol. Res. Pract. 205 (9) (2009) 626–633.
[75] T.J. Dudderidge, K. Stoeber, M. Loddo, G. Atkinson, T. Fanshawe, D.F. Griffiths, G.H. Williams, Mcm2, Geminin, and KI67 define proliferative state and are prognostic markers in renal cell carcinoma, Clin. Cancer Res. 11 (7) (2005) 2510–2517.
[76] M. Loddo, S.R. Kingsbury, M. Rashid, I. Proctor, C. Holt, J. Young, S. El-Sheikh, M. Falzon, K.L. Eward, T. Prevost, R. Sainsbury, K. Stoeber, G.H. Williams, Cell-cycle-phase progression analysis identifies unique phenotypes of major prognostic and predictive significance in breast cancer, Br. J. Cancer 100 (6) (2009) 959–970.
[77] J.A. Wohlschlegel, J.L. Kutok, A.P. Weng, A. Dutta, Expression of geminin as a marker of cell proliferation in normal tissues and malignancies, Am. J. Pathol. 161 (1) (2002) 267–273.
[78] R.G. Forsyth, G. De Boeck, S. Bekaert, T. De Meyer, A.H. Taminiau, D. Uyttendaele, H. Roels, M.M. Praet, P.C. Hogendoorn, Telomere biology in giant cell tumour of bone, J. Pathol. 214 (5) (2008) 555–563.
[79] L. De Boer, V. Oakes, H. Beamish, N. Giles, F. Stevens, M. Somodevilla-Torres, C. DeSouza, B. Gabrielli, Cyclin A/cdk2 coordinates centrosomal and nuclear mitotic events, Oncogene 27 (31) (2008) 4261–4268.
[80] M.A. Gonzalez, K.E. Tachibana, R.A. Laskey, N. Coleman, Control of DNA replication and its potential clinical exploitation, Nat. Rev. Cancer 5 (2) (2005) 135–141.
[81] E.W. Steyerberg, M. Schemper, F.E. Harrell, Logistic regression modeling and the number of events per variable: selection bias dominates, J. Clin. Epidemiol. 64 (12) (2011) 1464–1465 (author reply 1463-4).
[82] L. Molendini, M.S. Benassi, G. Magagnoli, M. Merli, M.R. Sollazzo, P. Ragazzini, G. Gamberi, C. Ferrari, A. Balladelli, P. Bacchini, P. Picci, Prognostic significance of cyclin expression in human osteosarcoma, Int. J. Oncol. 12 (5) (1998) 1007–1011.
[83] K. Yoshida, N. Oyaizu, A. Dutta, I. Inoue, The destruction box of human Geminin is critical for proliferation and tumor growth in human colon cancer cells, Oncogene 23 (1) (2004) 58–70.
[84] M.A. Gonzalez, K.E. Tachibana, S.F. Chin, G. Callagy, M.A. Madine, S.L. Vowler, S.E. Pinder, R.A. Laskey, N. Coleman, Geminin predicts adverse clinical outcome in breast cancer by reflecting cell-cycle progression, J. Pathol. 204 (2) (2004) 121–130.
[85] P. Shrestha, T. Saito, S. Hama, M.T. Arifin, Y. Kajiwara, F. Yamasaki, T. Hidaka, K. Sugiyama, K. Kurisu, Geminin: a good prognostic factor in high-grade astrocytic brain tumors, Cancer 109 (5) (2007) 949–956.
[86] D. Li, J. Zhang, Y. Li, J. Xia, Y. Yang, M. Ren, Y. Liao, S. Yu, X. Li, Y. Shen, Y. Zhang, Z. Yang, Surgery methods and soft tissue extension are the potential risk factors of local recurrence in giant cell tumor of bone, World J Surg Oncol 14 (2016) 114.